interact with DNA, although the main-chain atoms are occupied in the polar interactions between the loop and the two helical ends.

REFERENCES AND NOTES

1. P. C. Hanawalt, P. K. Cooper, A. K. Ganesan, C. A. Smith, *Annu. Rev. Biochem.* **48**, 783 (1979).
2. S. Yasuda and M. Sekiguchi, *Proc. Natl. Acad. Sci. U.S.A.* **67**, 1839 (1970).
3. E. C. Friedberg and J. J. King, *J. Bacteriol.* **106**, 500 (1971).
4. L. K. Gordon and W. A. Haseltine, *J. Biol. Chem.* **255**, 12047 (1980).
5. P. C. Seawell *et al.*, *J. Virol.* **35**, 790 (1980).
6. E. H. Radany and E. C. Friedberg, *Nature* **286**, 182 (1980).
7. S. McMillan *et al.*, *J. Virol.* **40**, 211 (1981).
8. Y. Nakabeppu and M. Sekiguchi, *Proc. Natl. Acad. Sci. U.S.A.* **78**, 2742 (1981).
9. H. R. Warner, L. M. Christensen, M.-L. Persson, *J. Virol.* **40**, 204 (1981).
10. Y. Nakabeppu, K. Yamashita, M. Sekiguchi, *J. Biol. Chem.* **257**, 2556 (1982).
11. E. A. Gruskin and R. S. Lloyd, *ibid.* **261**, 9607 (1986).
12. M. L. Dodson and R. S. Lloyd, *Mutation Res.* **218**, 49 (1989).
13. J. Kim and S. Linn, *Nucleic Acids Res.* **16**, 1135 (1988).
14. M. Monoharan, A. Mazamder, S. C. Ransom, J. A. Gerlt, P. H. Bolton, *J. Am. Chem. Soc.* **110**, 2690 (1988).
15. A. Mazumder *et al.*, *ibid.* **111**, 8029 (1989).
16. A. K. Ganesan, P. C. Seawell, R. J. Lewis, P. C. Hanawalt, *Biochemistry* **25**, 5751 (1986).
17. K. Morikawa, M. Tsujimoto, M. Ikehara, T. Inaoka, E. Ohtsuka, *J. Mol. Biol.* **202**, 683 (1988).
18. W. A. Hendrickson and J. H. Konnert, in *Computing in Crystallography*, R. Diamond, S. Ramaseshan, K. Venkatesan, Eds. (National Academy of Science of India, Bangolore, 1980), pp. 13.01–13.23.
19. W. Kabsch and C. Sander, *Biopolymers* **22**, 2577 (1983).
20. M. Levitt and C. Chochia, *Nature* **261**, 552 (1976).
21. Abbreviations for the amino acid residues are as follows: A, Ala; C, Cys; D, Asp; E, Glu; F, Phe; G, Gly; H, His; I, Ile; K, Lys; L, Leu; M, Met; N, Asn; P, Pro; Q, Gln; R, Arg; S, Ser; T, Thr; V, Val; W, Trp; and Y, Tyr.
22. T. Doi *et al.*, unpublished results.
23. H. Nakamura and S. Nishida, *J. Phys. Soc. Jpn.* **56**, 1609 (1987).
24. D. R. Dowd and R. S. Lloyd, *Biochemistry* **28**, 8699 (1989); *J. Mol. Biol.* **208**, 701 (1989).
25. A. Recinos III and R. S. Lloyd, *Biochemistry* **27**, 1832 (1988); D. G. Stump and R. S. Lloyd, *ibid.*, p. 1839; R. S. Lloyd and M. L. Augustine, *Proteins* **6**, 128 (1989); M. Ishida, Y. Kanamori, N. Hori, T. Inaoka, E. Ohtsuka, *Biochemistry* **29**, 3817 (1990).
26. W. Steigemann, thesis, Technische Universität, München (1974).
27. T. A. Jones, *J. Appl. Crystallogr.* **11**, 268 (1978).
28. J. P. Priestle, *ibid.* **21**, 572 (1988).

29. We are indebted to H. Nakamura for his help in molecular graphics work and A. Recktenwald for his collaboration in site-directed mutagenesis. Y. Ohta, T. Tanaka, S. Kimura, and H. Sakashita are acknowledged for their purification of T4 endonuclease V and M. Matsushima for his refinement of heavy-atom parameters. We also thank A. Klug, P. Evans, C. Chochia, J. Finch, and A. Pähler for their critical reading of the manuscript and helpful comments. Coordinates for the refined model of T4 endonuclease V have been submitted to the Protein Data Bank. This research was partly supported by a Human Frontier Science Program research grant for international collaboration groups.

8 November 1991; accepted 28 February 1992

Tertiary Structure Around the Guanosine-Binding Site of the *Tetrahymena* Ribozyme

Jin-Feng Wang and Thomas R. Cech*

A cleavage reagent directed to the active site of the *Tetrahymena* catalytic RNA was synthesized by derivatization of the guanosine substrate with a metal chelator. When complexed with iron(II), this reagent cleaved the RNA in five regions. Cleavage at adenosine 207, which is far from the guanosine-binding site in the primary and secondary structure, provides a constraint for the higher order folding of the RNA. This cleavage site constitutes physical evidence for a key feature of the Michel-Westhof model. Targeting a reactive entity to a specific site should be generally useful for determining proximity within folded RNA molecules or ribonucleoprotein complexes.

Many RNA molecules require specifically folded structures for their biological activity. RNA base-pairing interactions (secondary structure) can be established by sequence analysis of functionally equivalent RNAs from phylogenetically diverse organisms (*1*). In contrast, our understanding of the three-dimensional (3-D) structure of RNAs is limited. Only for some small RNAs have atomic-resolution structures been determined by x-ray crystallography or nuclear magnetic resonance spectrometry (*2*). Methods such as site-specific mutagenesis, chemical and enzymatic probing, and comparative sequence analysis have proven to be informative in studying other RNA 3-D structures. Ribozymes, or catalytic RNAs, are attractive for studies of RNA folding because their structure is directly reflected in their activity.

The L-21 Sca I ribozyme is derived from the group I intervening sequence of *Tetrahymena thermophila* pre–ribosomal RNA (*3*). This ribozyme cleaves other RNA molecules using as a nucleophile the 3′ hydroxyl of G (guanosine or one of its 5′-phosphorylated forms) [Fig. 1A; (*4*)]. The G264-C311 base pair (the G-site) binds the G substrate (*5*, *6*).

Howard Hughes Medical Institute, Department of Chemistry and Biochemistry, University of Colorado, Boulder, CO 80309–0215.

*To whom correspondence should be addressed.

We used affinity cleavage (cleavage by a bound reagent) to identify regions of the RNA in proximity to the G-site. The redox active metal iron(II) [Fe(II)], when chelated by EDTA or DTPA (diethylenetriaminepentaacetic acid) and incubated with a reducing reagent such as ascorbate in the presence of O_2 (or H_2O_2), generates short-lived free radicals that initiate oxidative degradation of any neighboring nucleic acid sugars (*7*). Cleavage is largely independent of base identity or secondary structure (*8*). Tethering EDTA-Fe(II) or DTPA-Fe(II) to guanosine 5′-phosphate (GMP) was expected to target the destructive reagent to the G-site, thereby providing information about the 3-D structure of the catalytic core of the ribozyme.

The metal chelator DTPA was tethered to the 5′ phosphate of GMP [G-DTPA, Fig. 1B; (*9*)], and its reactivity as a ribozyme substrate was compared to that of GMP. The G-DTPA reagent was active as a nucleophile and yielded the same product from 5′ end-labeled RNA substrate (Fig. 1A) as did GMP and guanosine (*10*).

When a mixture of G-DTPA and GMP was reacted with an internally labeled RNA substrate, both DTPA-Gp*AGU and Gp*AGU were formed at a ratio that represented the relative reactivity of the two G substrates (Fig. 2). The activity of G-DTPA was about one-tenth that of GMP. Quantitative kinetic measurements

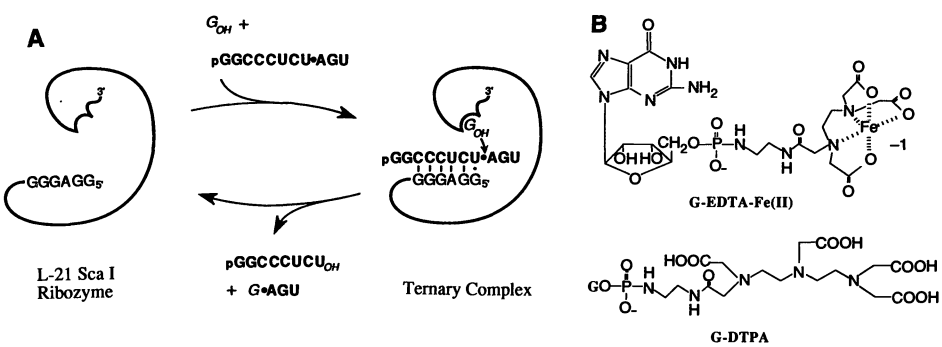

Fig. 1. (**A**) Endonuclease reaction catalyzed by the ribozyme. (**B**) Structures of GMP-EDTA-Fe(II) [G-EDTA-Fe(II)] and GMP-diethylenetriaminepentaacetic acid (G-DTPA).

(*11*) revealed that the k_{cat}/K_m for GMP was 4×10^5 M^{-1} min^{-1} and for G-DTPA was 4×10^4 M^{-1} min^{-1}. The k_{cat}/K_m is the second-order rate constant for the reaction between the ribozyme-substrate complex and GMP (or G-DTPA) and represents the binding of G and the subsequent chemical step. Thus, G-DTPA functions as a nucleophile nearly as well as does GMP in the ribozyme reaction (*11*).

When L-21 Sca I ribozyme was incubated with G-DTPA-Fe(II) and a reducing agent under conditions appropriate for ribozyme activity, two types of cleavage were observed (Fig. 3). The overall cleavage pattern was similar to that generated by solvent-based EDTA-Fe(II) (*12*). In addition, there were five regions of enhanced cleavage (*13*). The G-EDTA-Fe(II) reagent (Fig. 1B) gave the same cleavage pattern as did G-DTPA-Fe(II) (*10*).

To test whether the enhanced cleavage regions resulted from G-DTPA-Fe(II) bound at the G-site, the DTPA derivative of uridine monophosphate (U-DTPA) was tested as an Fe(II) complex for the cleavage of L-21 Sca I (Fig. 3). The U-DTPA is similar in structure to G-DTPA but does not bind specifically to the ribozyme. Cleavage of U-DTPA-Fe(II) was indistinguishable from that of EDTA-Fe(II), which was consistent with both reagents acting as solvent-based cleavage reagents. Five regions of cleavage specific to G-DTPA-Fe(II) were inhibited by GMP but not by uridine 5′-phosphate (Fig. 3B), as was expected if they were the result of G-DTPA occupying the G-site (*14*). These regions involved nucleotides 206 to 208, 262, 301

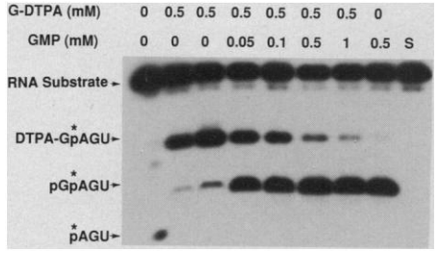

Fig. 2. Activity of G-DTPA as a nucleophile in the ribozyme-catalyzed endonuclease reaction. L-21 Sca I ribozyme (100 nM) was incubated for 10 min at 42°C, in 10 mM $MgCl_2$, 60 mM tris, pH 7.5, and reacted with the substrate pppGGCCCUCUp*AGU (~20 nM) for 1.5 min (leftmost lane); p*AGU is the product of this ribozyme-catalyzed hydrolysis. Other reactions contained G-DTPA and GMP as indicated. Lane S shows the unreacted RNA substrate. The third lane shows the same reaction as in the second lane but with 120 nM L-21 Sca I from another preparation. DTPA-Gp*AGU and pGp*AGU are products of the reactions with G-DTPA and GMP, respectively. Reactions were analyzed by electrophoresis on a denaturing 20% polyacrylamide gel.

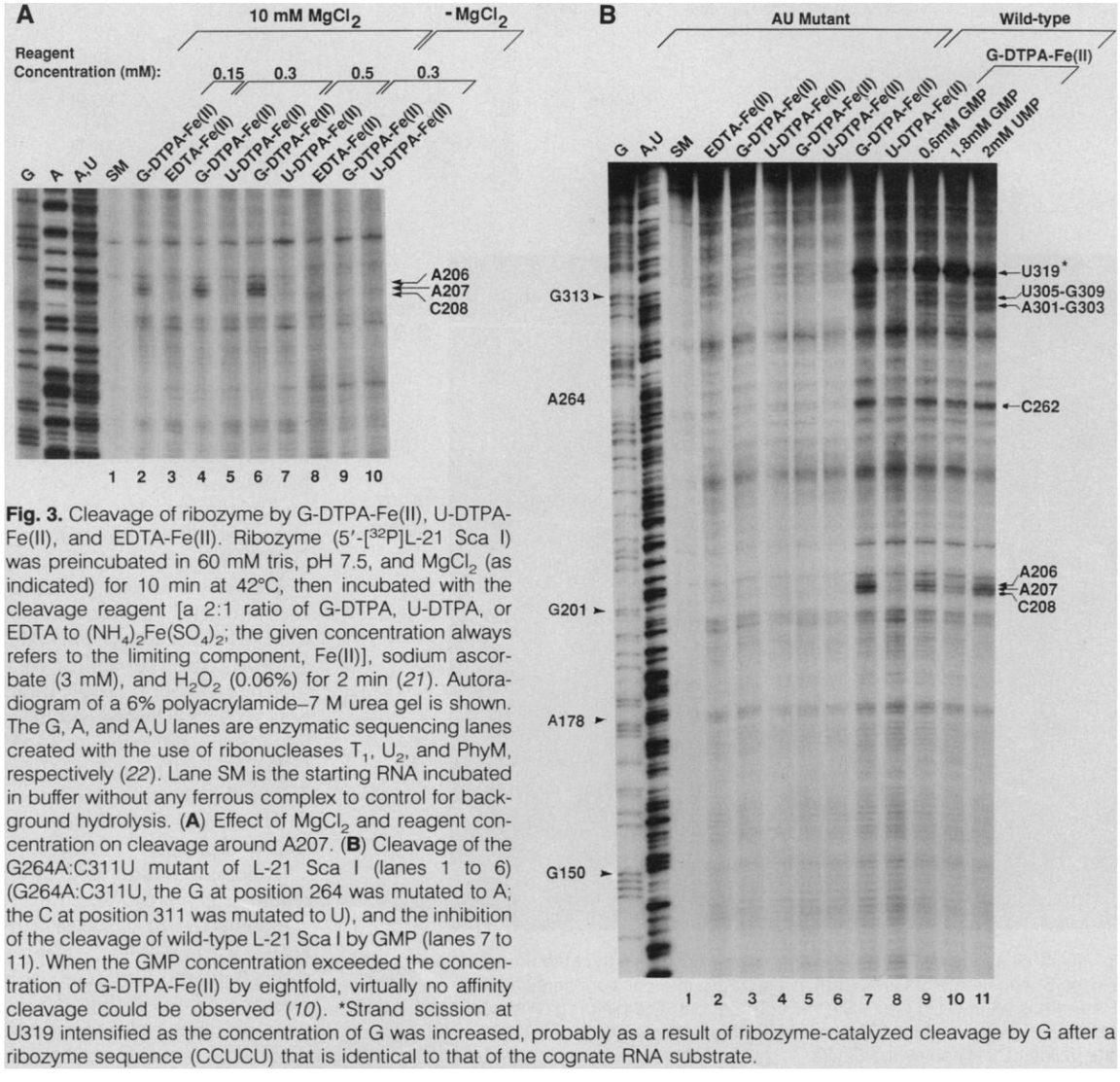

Fig. 3. Cleavage of ribozyme by G-DTPA-Fe(II), U-DTPA-Fe(II), and EDTA-Fe(II). Ribozyme (5′-[^{32}P]L-21 Sca I) was preincubated in 60 mM tris, pH 7.5, and $MgCl_2$ (as indicated) for 10 min at 42°C, then incubated with the cleavage reagent [a 2:1 ratio of G-DTPA, U-DTPA, or EDTA to $(NH_4)_2Fe(SO_4)_2$; the given concentration always refers to the limiting component, Fe(II)], sodium ascorbate (3 mM), and H_2O_2 (0.06%) for 2 min (*21*). Autoradiogram of a 6% polyacrylamide–7 M urea gel is shown. The G, A, and A,U lanes are enzymatic sequencing lanes created with the use of ribonucleases T_1, U_2, and PhyM, respectively (*22*). Lane SM is the starting RNA incubated in buffer without any ferrous complex to control for background hydrolysis. (**A**) Effect of $MgCl_2$ and reagent concentration on cleavage around A207. (**B**) Cleavage of the G264A:C311U mutant of L-21 Sca I (lanes 1 to 6) (G264A:C311U, the G at position 264 was mutated to A; the C at position 311 was mutated to U), and the inhibition of the cleavage of wild-type L-21 Sca I by GMP (lanes 7 to 11). When the GMP concentration exceeded the concentration of G-DTPA-Fe(II) by eightfold, virtually no affinity cleavage could be observed (*10*). *Strand scission at U319 intensified as the concentration of G was increased, probably as a result of ribozyme-catalyzed cleavage by G after a ribozyme sequence (CCUCU) that is identical to that of the cognate RNA substrate.

Fig. 4. Regions of cleavage of L-21 Sca I RNA by bound G-DTPA-Fe(II) and by solvent-based Fe(II) reagents, superimposed onto the secondary structure diagram of the RNA (*17*). Arrows, nucleotide positions of enhanced cleavage by G-DTPA-Fe(II) relative to U-DTPA-Fe(II). The lengths of arrows represent qualitatively the relative cleavage intensities at the indicated nucleotides. Not shown is the cleavage at C262, which was not quantitated because of adjacent background bands. The shaded areas indicate protection from cleavage by solvent-based EDTA-Fe(II) in the presence of $MgCl_2$ (*12*); these regions were also protected from solvent-based G-DTPA-Fe(II) and U-DTPA-Fe(II) cleavage in the present study.

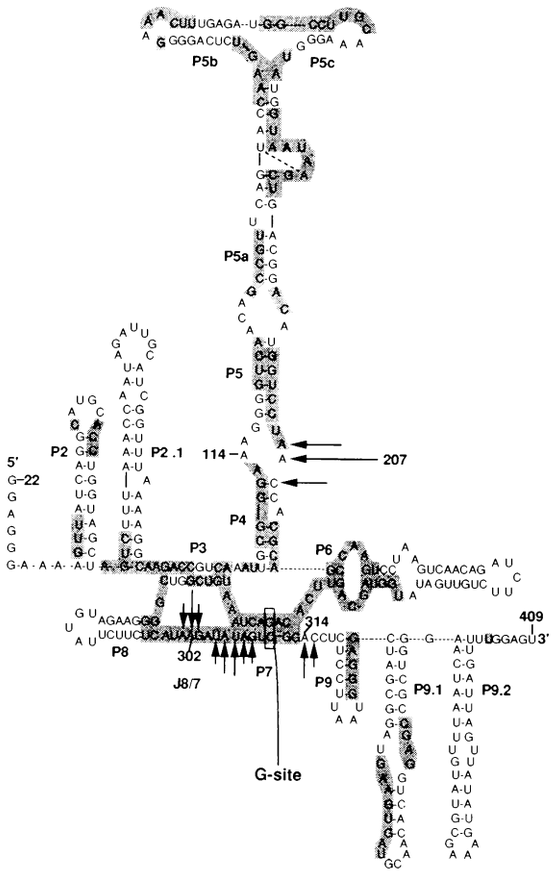

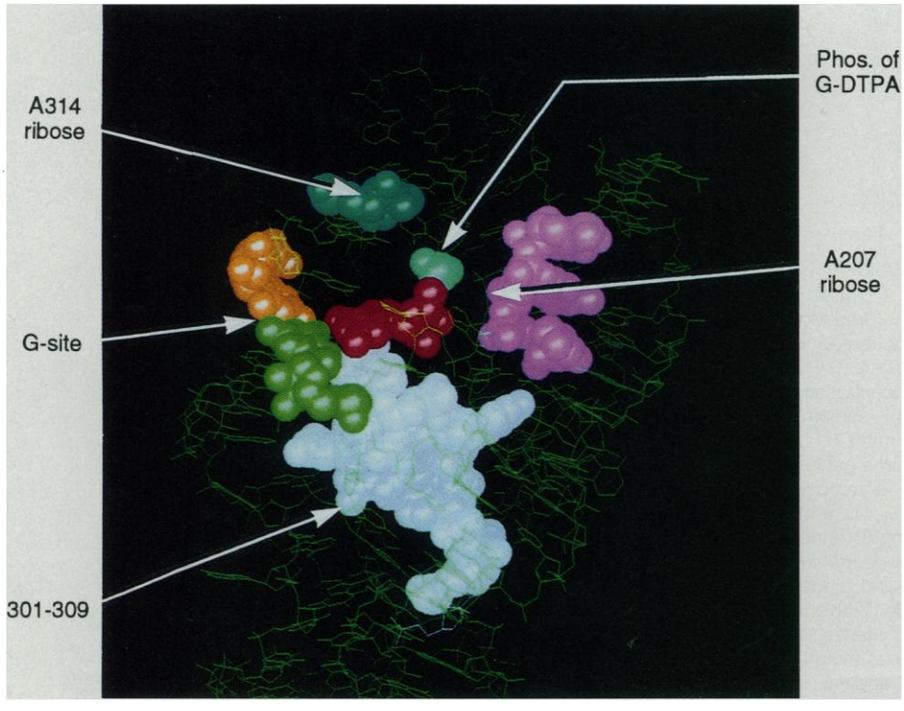

Fig. 5. Sites of affinity cleavage by G-DTPA-Fe(II) superimposed onto the M-W model (*17*). The light blue residue is the 5′ phosphate of G414 (red), presumably in a position identical to the phosphate to which DTPA-Fe(II) is tethered in the G-DTPA-Fe(II) reagent. The pink region shows A206, A207, and C208; the dark blue represents A314; the white region shows A301 to G309; and the green (G264) and the yellow (C311) show the G-site.

Table 1. Distances from 5′ phosphate of bound GMP to other nucleotides in the *Tetrahymena* ribozyme according to the model of Michel and Westhof (*17*). The distance is measured between the 5′ phosphate of GMP occupying the G-site and the 4′ carbon of the other nucleotide; the 4′ carbon is likely the primary target of the reactive species generated by G-DTPA-Fe(II), which initiates strand scission (*8*). DTPA was tethered to the 5′ phosphate through a flexible ethylene chain (Fig. 1B), and the maximum distance of the 5′ phosphate to the Fe(II) in G-DTPA-Fe(II) is ~10 Å. The asterisks indicate that there are residues between these nucleotides and the 5′ phosphate of GMP that are expected to attenuate the cleavage intensity. The number of pluses in the cleavage column represents the G-DTPA-Fe(II) cleavage intensity. ++ is about 50% of +++, and + is about 25% of +++, as determined with the PhosphorImager (Molecular Dynamics). (+), Cleavage was not quantitated.

Nucleotide	Distance (Å)	Cleavage
U205	17.2*	–
A206	11.2	++
A207	7.0	+++
C208	10.6	++
C209	16.5	–
C262	12.1	(+)
U300	35.6*	–
A301	32.2*	+
A302	26.9*	++
G303	21.6*	+
A304	18.1	–
U305	14.5	+
A306	13.2	++
U307	17.2*	++
A308	15.2	+
G309	15.8	+
G313	14.9	–
A314	15.7	+
C315	Not modeled	+
G264	17.9	–
C311	16.9	–

to 303, 305 to 309, and 314 to 315 (see below).

To confirm that the observed affinity cleavages all resulted from binding of G-DTPA-Fe(II) to the known G-site, we performed cleavage reactions with the G264A:C311U double mutant (Fig. 3B) of the L-21 Sca I RNA. This AU mutant has a greatly reduced ability to use G as a substrate (*5*) but is largely intact structurally (*15*). The cleavage pattern with the AU mutant was the same for G-DTPA-Fe(II), U-DTPA-Fe(II), and EDTA-Fe(II) (Fig. 3B), indicating that binding of G-DTPA-Fe(II) to the G-site accounts for all the affinity cleavages.

Ribozyme folding and catalytic activity require Mg^{2+} (*16*). When L-21 Sca I RNA was subjected to cleavage with G-DTPA-Fe(II) without Mg^{2+}, cleavage occurred throughout the molecule, with no affinity cleavage observed (Fig. 3A). The dependence of affinity cleavage on Mg^{2+} implies that the cleavage resulted from the properly

folded structure of the ribozyme.

The positions of cleavage were mapped by high resolution polyacrylamide gel electrophoresis by comparison to standard sequencing ladders. Sites around nucleotides 206 to 208 were mapped with 5′ end-labeled RNA (Fig. 3), and those around 301 to 315 with 3′ end-labeled RNA (*10*). Points of affinity cleavage are represented by arrows on the secondary structure diagram (Fig. 4). Some of these sites (for example, A207) are far from the G-site in the secondary structure, but we infer that they are close to the 5′ end of bound GMP in the 3-D structure. All five affinity cleavage regions resided within the catalytic core of the ribozyme (*17, 18*).

Because our experimental results are independent of any theoretical model for the 3-D structure of the catalytic center, they provide a test for such models and constraints for building new models. The identification of the most prominent cleavage site at the backbone of A207 as being close to the 5′ end of GMP bound at the G-site provides a structural constraint for the overall architecture of the folded RNA. It is possible that the backbone around A207 might even form part of the G-site.

A model for the 3-D structure of the conserved catalytic core of group I introns has been developed [Michel-Westhof (M-W) model, (*17*)], mainly on the basis of comparative sequence analysis and stereochemical modeling. Our observation of affinity cleavages in the regions of A207, C262, and A314 supports this model. In the M-W model, the backbones of nucleotides A206, A207, and C208 are the groups most proximal to the 5′ moiety of G (Fig. 5 and Table 1) and, therefore, should be the most exposed to attack by the reactive species generated from G-DTPA-Fe(II). The backbone of A314 is not as close to the 5′ end of G as any of the above three nucleotides, but it is still within a reasonable distance to be reached by a diffusible reactive species. It is then expected from the model that cleavage at A314 would be observed but to a lesser extent. This is confirmed by the experimental result.

The lack of affinity cleavage at the G-site is also consistent with the model. The backbones of G264 and C311 in the model are farther from the 5′ moiety of G than the backbone of nucleotides in the A207 or A314 regions of cleavage. The amount of affinity cleavage at G264 or C311 should thus be lower than the amount of cleavage at A314.

There is apparent discrepancy between the M-W model and the observed affinity cleavage in the J8/7 region around A302 and U307. In the M-W model, the backbone around A302 and U307 is up to 32 Å away from the 5′ moiety of G (Table 1), which does not lead to the prediction of affinity cleavages at these sites. Furthermore, even if the G were closer to the J8/7 region than pictured in the model, the observed pattern of cleavage at A302 and U307 with no cleavage at A304 would not be expected from the model. Instead, this cleavage pattern is consistent with a V-shaped structure for the J8/7 region with bending at A304. It is possible that a subpopulation of the molecules has a conformation that brings J8/7 close to the G-site (*19*). If only a single conformer exists, then a modification of the M-W model in the J8/7 region as well as its position relative to the G site is required to accommodate the experimental data.

It is possible to derivatize a small oligonucleotide with a metal chelator and incorporate it at a site of interest in an RNA molecule with the use of ligase technology (*20*). Thus, the approach of targeting a reactive group at a specific site and then mapping the nucleotides in proximity to that site offers a general method for studying complex RNA or ribonucleoprotein 3-D structures.

REFERENCES AND NOTES

1. H. F. Noller and C. R. Woese, *Science* **212**, 403 (1981).
2. S.-H. Kim *et al.*, *ibid.* **185**, 435 (1974); J. D. Robertus *et al.*, *Nature* **250**, 546 (1974); S. R. Holbrook, C. Cheong, I. Tinoco, Jr., S.-H. Kim, *ibid.* **353**, 579 (1991); H. A. Heus and A. Pardi, *Science* **253**, 191 (1991).
3. A. J. Zaug, C. A. Grosshans, T. R. Cech, *Biochemistry* **27**, 8924 (1988).
4. T. R. Cech, *Science* **236**, 1532 (1987); *Annu. Rev. Biochem.* **59**, 543 (1990); B. L. Bass and T. R. Cech, *Nature* **308**, 820 (1984).
5. F. Michel, M. Hanna, R. Green, D. P. Bartel, J. W. Szostak, *Nature* **342**, 391 (1989).
6. M. Yarus, M. Illangesekare, E. Christian, *J. Mol. Biol.* **222**, 995 (1991); M. D. Been and A. T. Perrotta, *Science* **252**, 434 (1991).
7. C. Walling, *Acc. Chem. Res.* **8**, 125 (1975); J. Stubbe and J. W. Kozarich, *Chem. Rev.* **87**, 1107 (1987); J. S. Taylor, P. G. Schultz, P. B. Dervan, *Tetrahedron* **40**, 457 (1984).
8. R. Hertzberg and P. B. Dervan, *Biochemistry* **23**, 3934 (1984); T. D. Tullius *et al.*, *Methods Enzymol.* **155**, 537 (1987); D. W. Celander and T. R. Cech, *Biochemistry* **29**, 1355 (1990); T. M. Lohman, *ibid.*, p. 5220.
9. M. G. Ivanovskaya, M. B. Gottikh, Z. A. Shabarova, *Nucleosides Nucleotides* **6**, 913 (1987); D. J. Hnatowich, W. W. Layne, R. L. Childs, *Int. J. Appl. Radiat. Isot.* **33**, 327 (1982); B. C. F. Chu and L. E. Orgel, *Proc. Natl. Acad. Sci. U.S.A.* **82**, 963 (1985).
10. J.-F. Wang and T. R. Cech, unpublished data.
11. Single-turnover reactions for measuring k_{cat}/K_m for G with RNA substrate 5′-[^{32}P]GGCCCUCUA$_5$ were as described [D. Herschlag, J. A. Piccirilli, T. R. Cech, *Biochemistry* **30**, 4844 (1991)] except at 42°C. Concentrations of GMP were 0, 0.5, 1, and 1.5 μM and concentrations of G-DTPA were 0, 0.5, 1, 1.5, 2, 4, 6, and 8 μM. With the DNA substrate 5′-[^{32}P]deoxy(GGCCCUCUA), where k_{cat} and K_m could be measured separately (*23*), G-DTPA and GMP gave indistinguishable values of these kinetic parameters (*10*). The DNA cleavage was performed at 50 mM Mg^{2+} rather than 10 mM Mg^{2+} because faster reaction at 50 mM Mg^{2+} facilitated the experiments.
12. J. A. Latham and T. R. Cech, *Science* **245**, 276 (1989); T. S. Heuer, P. S. Chandry, M. Belfort, D. W. Celander, T. R. Cech, *Proc. Natl. Acad. Sci. U.S.A.* **88**, 11105 (1991).
13. When the concentration of Fe(II) exceeded that of metal chelator, Fe(II) initiated a third type of specific cleavage of the ribozyme (*10*). The chemical mechanism for this type of cleavage is probably similar to that of EDTA-Fe(II), with the sites of cleavage being determined by Fe(II) binding sites in the RNA 3-D structure. Magnesium ion was a strong inhibitor of the cleavage by Fe(II). However, moderate cleavage was still observed at 10 mM Mg^{2+} with only 5 μM of Fe(II), suggesting the existence of sites where Fe(II) binds with much higher affinity than Mg^{2+}. It remains to be seen to what extent the Fe(II) sites overlap with the Mg(II) sites involved in the folding and catalysis of the ribozyme.
14. Competition of G-DTPA-Fe(II) cleavage on addition of GMP was quantitated by PhosphorImager analysis. Competition occurred in the concentration range expected from the known dissociation constant for G [~0.3 mM at 30°C and ~1 mM at 50°C; (*23*)].
15. The structure integrity of the mutant was judged by its equilibrium constant for binding RNA oligonucleotides [A. M. Pyle, J. A. McSwiggen, T. R. Cech, *Proc. Natl. Acad. Sci. U.S.A.* **87**, 8187 (1990)] and by its activity with *2*-aminopurine ribonucleoside as a substrate and direct structure mapping [T. R. Cech, D. W. Celander, P. Legault, D. Herschlag, unpublished data; see also (*5*)].
16. C. A. Grosshans and T. R. Cech, *Biochemistry* **28**, 6888 (1989); D. W. Celander and T. R. Cech, *Science* **251**, 401 (1991).
17. F. Michel and E. Westhof, *J. Mol. Biol.* **216**, 585 (1990).
18. T. R. Cech, *Gene* **73**, 259 (1988); M. D. Been *et al.*, *Cold Spring Harbor Symp. Quant. Biol.* **LII**, 147 (1988); S. Couture *et al.*, *J. Mol. Biol.* **215**, 345 (1990).
19. Although a previous kinetic study indicated that almost all the L-21 Sca I molecules in solution were enzymatically active as a single species [D. Herschlag and T. R. Cech, *Biochemistry* **29**, 10159 (1990)], considering the detection sensitivity of the kinetic assay it is still feasible that a small percentage (for example, 20%) of the population exists in other conformations.
20. A. G. Bruce and O. Uhlenbeck, *Biochemistry* **21**, 855 (1982); M. J. Moore and P. A. Sharp, *Science*, in press.
21. The same results as those in Fig. 3 were obtained when the reactions were performed aerobically for 90 min without H_2O_2. The reactions were quenched by addition of an equal volume of loading buffer [10 M urea, 0.2× TBE (1× TBE: 100 mM tris, 100 mM boric acid, 2 mM EDTA; pH 8.3), 0.02% bromophenol blue and xylene cyanol, 40 mM EDTA, and 20 mM thiourea].
22. The assignment of cleavage product identity with the 5′ end-labeled RNA was shifted one nucleotide 5′ of the enzymatic cleavage product because the strand scission by EDTA-Fe(II) is accompanied by elimination of the ribose moiety (*8*).
23. D. Herschlag and T. R. Cech, *Nature* **344**, 405 (1990).

24. We thank J. A. Latham for initiating the affinity cleavage approach in this laboratory and for discussions thereafter; L. Weinstein, D. Herschlag, and J. A. Piccirilli for comments on the manuscript; and the W. M. Keck Foundation for support of RNA science on the Boulder campus. T.R.C. is an Investigator and J.-F.W. is an Associate of the Howard Hughes Medical Institute.

9 January 1992; accepted 12 March 1992